JOURNAL OF TISSUE ENGINEERING AND REGENERATIVE MEDICINE
J Tissue Eng Regen Med 2015; **9**: 641–645.
Published online 12 February 2013 in Wiley Online Library (wileyonlinelibrary.com) **DOI:** 10.1002/term.1687

SHORT COMMUNICATION

Motility imaging via optical coherence phase microscopy enables label-free monitoring of tissue growth and viability in 3D tissue-engineering scaffolds

Christina Holmes[1], Maryam Tabrizian[1,2] and Pierre O. Bagnaninchi[3]*
[1]*Department of Biomedical Engineering, McGill University, Montreal, Canada*
[2]*Faculty of Dentistry, McGill University, Montreal, Canada*
[3]*MRC Centre for Regenerative Medicine, University of Edinburgh, UK*

Abstract

As the field of tissue engineering continues to progress, there is a deep need for non-invasive, label-free imaging technologies that can monitor tissue growth and health within thick three-dimensional (3D) constructs. Amongst the many imaging modalities under investigation, optical coherence tomography (OCT) has emerged as a promising tool, enabling non-destructive *in situ* characterization of scaffolds and engineered tissues. However, the lack of optical contrast between cells and scaffold materials using this technique remains a challenge. In this communication, we show that mapping the optical phase fluctuations resulting from cellular viability and motility allows for the distinction of live cells from their surrounding scaffold environment. Motility imaging was performed via a common-path optical coherence phase microscope (OCPM), an OCT modality that has been shown to be sensitive to nanometer-level fluctuations. More specifically, we examined the development of human adipose-derived stem cells and/or murine pre-osteoblasts within two distinct scaffold systems, commercially available alginate sponges and custom-microfabricated poly(D,L-lactic-co-glycolic acid) fibrous scaffolds. Cellular motility is demonstrated as an endogenous source of contrast for OCPM, enabling real-time, label-free monitoring of 3D engineered tissue development.

Received 26 June 2012; Revised 10 September 2012; Accepted 23 November 2012

Keywords **tissue engineering; optical coherence tomography; cell viability; micromotion; phase fluctuation; scaffold**

The development of non-invasive, label-free three-dimensional (3D) imaging technologies is vital to the future progress of tissue engineering and regenerative medicine. Assessment of *in vitro* engineered tissues requires accurate monitoring of tissue growth, morphology, viability and bioactivity over time within 3D constructs. This challenge becomes even greater when one considers the thickness of the tissue constructs, the need for high imaging resolution and the wide variety of cell types and scaffolding materials involved. As no one method can currently meet all these criteria, a combination of different techniques is typically used to evaluate various aspects of engineered tissue structure and health (Smith *et al.*, 2010a). The majority of these procedures are destructive end-point tests, such as histology, scanning electron microscopy (SEM), immunohistochemistry and metabolic assays. These require the use of staining agents and sample processing and sectioning, thus preventing time-course studies and requiring numerous samples at great cost. The few techniques that do allow for real-time monitoring, such as

*Correspondence to: P. O. Bagnaninchi, MRC Centre for Regenerative Medicine, University of Edinburgh, Edinburgh EH16 4SB, UK. E-mail: pierre.bagnaninchi@ed.ac.uk

confocal microscopy, are either limited in imaging penetration depth to a few hundred micrometres and/or require fluorescent labelling.

Optical coherence tomography (OCT) is an interferometric imaging modality (Huang *et al*., 1991; Fujimoto *et al*., 1995) that has emerged as a promising tool for 3D monitoring of engineered tissues. Achieving micrometre-scale resolution at millimetre-scale penetration depths, OCT has been established as a clinical standard in ophthalmology (Drexler *et al*., 2001), with further medical applications under investigation in the areas of dermatology, oncology and cardiology (Boppart *et al*., 1998; Fujimoto, 2003). Operating under a principle similar to ultrasound imaging, with the exception of measuring delays in backscattered light instead of sound, OCT enables non-invasive, real-time, label-free imaging both *in vitro* and *in vivo* (Fujimoto, 2003).

In the field of tissue engineering, OCT has been used to characterize scaffold architecture and porosity as well as to assess cell seeding, growth and migration within hydrogels and scaffolds (Ahearne *et al*., 2008; Bagnaninchi *et al*., 2007; Yang *et al*., 2006; Liang *et al*., 2009; Tan *et al*., 2006; Smith *et al*., 2010b). However, with the exception of optically clear hydrogels, no clear optical contrast exists between cells and surrounding scaffold materials via OCT imaging.

One OCT variant, known as spectral domain optical coherence phase microscopy (OCPM), can achieve quantitative phase-contrast images that enable single-cell mapping and the detection of nanometer-level fluctuations (Choma *et al*., 2005). Recently, we developed a common-path optical coherence phase microscopy system with a sensitivity that enabled the recording of phase fluctuations associated with motility of viable cells in two dimensions (2D) and 3D (Bagnaninchi *et al*., 2011). Similarly, Dunkers *et al*. (2012) monitored cell viability with optical coherence microscopy via measurement of intensity speckle fluctuation. Finally, Nolte and colleagues used digital holographic optical coherence imaging to record optical fluctuations in multicellular tumour spheroids, and demonstrated that these fluctuations arise from cellular and intracellular motility (Jeong *et al*., 2007; Nolte *et al*., 2011).

Here we demonstrate that the optical fluctuations arising from the motility of live cells can be used as an endogeneous source of contrast between cells and surrounding scaffold materials. We performed OCPM motility imaging in 3D for a variety of engineered tissues, utilizing two distinct scaffold systems with different architectures and two cell types. Our results show that motility imaging enables label-free, non-invasive monitoring of cell growth and viability within various polymeric scaffold systems.

The OCPM system used in this study (Figure 1a) was in a common path set-up, utilizing a strong reflection within the sample arm as a reference, rather than a separate reference arm, as in a conventional Michelson interferometer. This resulted in an increase in phase stability, as common noise was rejected more efficiently. The system, as described previously (Bagnaninchi *et al*., 2011), was based upon a commercial OCT engine (Callisto, Thorlabs) with a superluminescent diode (SLD) light source centred at 930 nm, with a FWHM bandwidth of 90 nm, providing a tissue resolution of approximately 5 μm. The light was coupled out of the OCT engine into a single-mode fibre and collimated onto a pair of galvanometers for raster scanning. The custom laser scanning head (LSH) was attached to an inverted microscope (SPi95, Brunel) and delivered to a custom scanning lens. A spectrum was measured at each x,y point of the sample at a rate of 1200 spectra/s, with 500 A scans collected in the x direction. Fast Fourier transform of the spectra yielded both intensity and phase information along the depth, z. Intensity data were used to perform in-depth microstructural imaging. In addition, we recorded phase fluctuation measurements by collecting several successive B scans at the same location, and the maximum and standard deviation of the first-time derivative of the phase, i.e. time fluctuations, were analysed over the acquisition time interval.

Cell growth and viability were imaged and analysed in two polymeric scaffold systems with very different architectures. One was a commercially available alginate sponge, Algimatrix (Gibco), with a pore size range of 50–200 μm. The other was a custom-microfabricated fibrous poly(D,L-lactic-co-glycolic acid) scaffold, described previously (Daoud *et al*., 2011), with a layered mesh-like structure and an average pore size of approximately 260 μm. Two different cell types were employed in these scaffold-seeding experiments: human adipose-derived stem cells (ADSCs; Invitrogen) cultured in low-serum MesenPRO RS medium, supplemented with 2 mM L-glutamine and MesenPRO RS growth supplements (Invitrogen); and murine MC3T3-E1 pre-osteoblasts (ATCC) grown in α-minimum essential medium (α-MEM) supplemented with 10% fetal bovine serum (FBS), 1% penicillin/streptomycin and 2 mM L-glutamine (Invitrogen). Both cell lines were incubated at 37°C in a humidified atmosphere of 5% CO_2 until seeded onto scaffolds.

Algimatrix scaffolds in 96-well tissue culture plates were conditioned overnight in ADSC medium and statically seeded with ADSCs, according to manufacturer protocols, at a density of 3×10^5 cells/scaffold in a volume of 100 μl ADSC medium supplemented with 10% v/v Algimatrix Firming Buffer (Gibco). After 10 min of incubation, a further 100 μl ADSC medium without firming buffer was added to each well. The next day, the cell-seeded scaffolds were transferred to a non-adherent 24-well plate and 1 ml fresh ADSC medium was added.

Meanwhile, PLGA scaffolds were sterilized prior to cell seeding by immersion in 70% ethanol for 30 min, followed by two rinses in phosphate-buffered saline (PBS) and subsequent UV irradiation for 30 min. PLGA scaffolds in non-adherent 24-well plates were also conditioned overnight in either ADSC or MC3T3 media and subsequently seeded with either ADSCs or MC3T3s at a density of 1×10^6 cells/scaffold in a volume of 50 μl of the appropriate medium. After 4 h of incubation, a further 1.5 ml of the appropriate medium was added to each well.

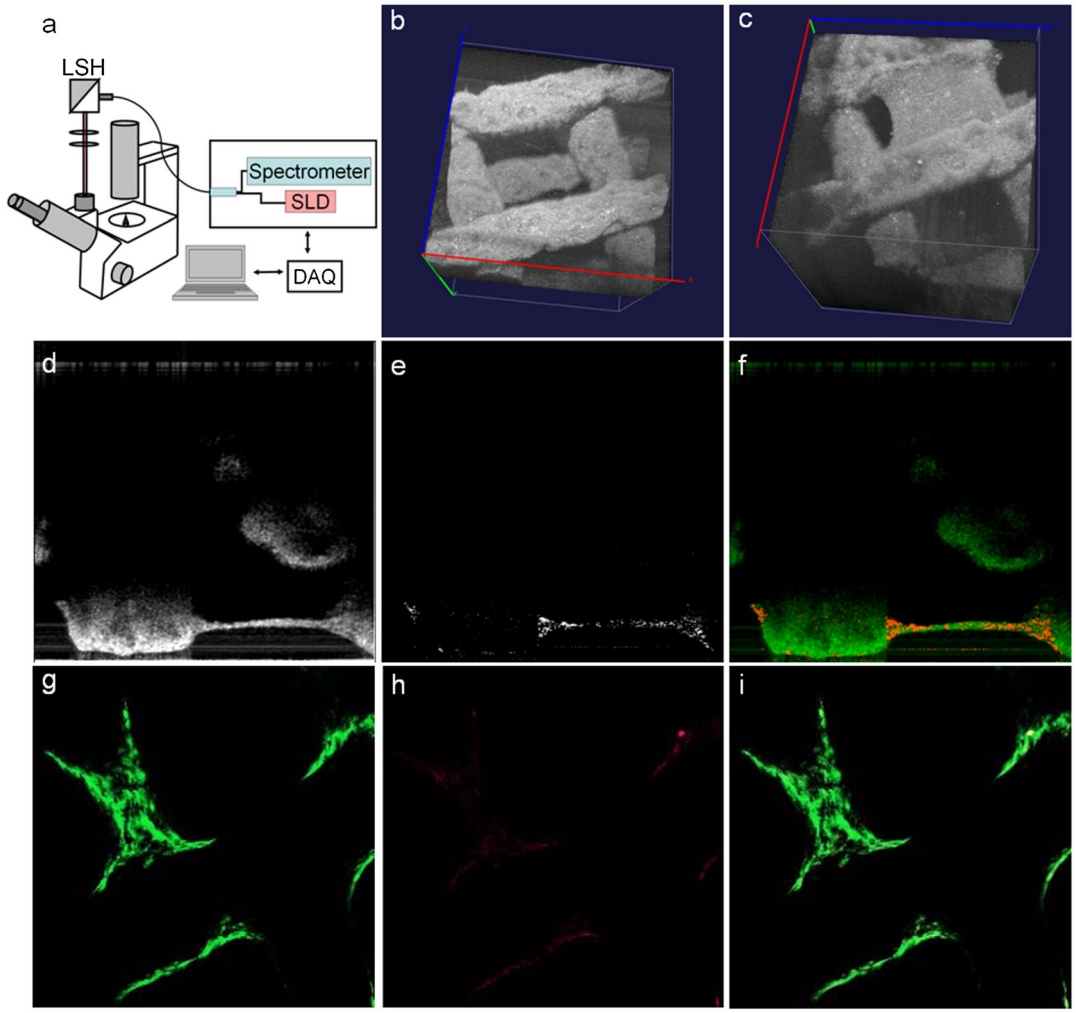

Figure 1. (a) Schematic of the optical coherence phase microscope (OCPM) in inverted mode. OCPM produces 1 mm^3 3D pictures of scaffolds by acquiring successive cross-sectional images by laser scanning from beneath the sample. (b) A PLGA printed scaffold seeded with MC3T3 cells at day 1 and (c) at day 7; at day 7 cells started to create a tissue-like structure. (d) Corresponding 1 × 1 mm cross-sectional image (*x*–*z*) in intensity mode. No contrast was observed between the cells and the scaffold. (e) Phase fluctuation imaging highlighted the cell layer. (f) Cell motility imaging is produced by combining the intensity mode on the green channel and phase fluctuation imaging mode on the red channel. Cell motility is an endogenous source of contrast that enables label-free and non-invasive monitoring of live cells within 3D scaffolds. (g–i) Live/dead (calcein/ethidium) confocal images of MC3T3 cells after 7 days of growth on PLGA printed scaffolds. Scaffolds were imaged from beneath the sample to a depth of around 100 μm, using a ×10 objective; scan size was approximately 1 × 1 mm (*x*–*y*). (g) Live, calcein-stained, image. (h) Dead, ethidium bromide-stained, image. (i) A merged image of the two channels

The following day, cell-seeded scaffolds were transferred to a fresh non-adherent 24-well plate and 1.5 ml of fresh medium was added. Both types of scaffolds were cultured for a period of at least 7 days, with medium exchanges performed every other day.

Cell growth and viability within PLGA and Algimatrix scaffolds were monitored over time via OCPM scans performed every other day. 3D images of a 1 mm^3 volume of scaffold morphology were produced by acquiring successive cross-sectional 2D scans via laser scanning. Looking only at the 3D light intensity images of MC3T3 growth in PLGA scaffolds on days 1 (Figure 1b) and 7 (Figure 1c), changes in construct morphology over time are evident.

On the first day, the underlying mesh-like 3D structure of the fibrous scaffold is quite clear. In places one can even discern the micro-porosity, due to salt-leaching, within the polymeric strands themselves. Meanwhile, at this early time point it is difficult to distinguish the pre-osteoblast cells from the polymeric strands on which they are growing, as the image contrast between the two is low. The cells at this stage are mostly apparent as small bulges around the strands. By contrast, at day 7 the gaps between polymer strands are becoming filled with tissue sheets and projections, indicating substantial cell growth. Although there is much higher tissue volume at this stage, when one observes a 2D cross-sectional light intensity scan of the same scaffold (Figure 1d), there is still very low contrast between the cells and the polymeric material, making it particularly difficult to discern the cells where they are attached to the strands. The phase fluctuation scans of that same region of the scaffold (Figure 1e), however, render the cell layer apparent. By overlaying the intensity image (green channel, Figure 1f)

and the phase fluctuation image (red channel, Figure 1f), we can map cell viability/motility to tissue morphology without the need for additional instrumentation or contrast agents.

In order to confirm that the cells scanned via OCPM were viable, day 7 MC3T3-seeded PLGA scaffolds were stained with calcein-AM and ethidium homodimer-1 (Live/Dead® Viability/Cytotoxicity Kit, Invitrogen, Canada) to label live and dead cells, respectively. Live/dead cell imaging was performed to a depth of approximately 100 μm, using a Zeiss LSM 510 confocal microscope. A representative series of images (Figure 1g–i) indicates that, while there is some cell death within these scaffolds, most MC3T3 pre-osteoblasts remained viable.

Using ADSCs, we have previously shown that the phase fluctuations recorded via OCPM likely correspond to nanometre-scale micromotion associated with viable cells (Bagnaninchi *et al.*, 2011). In order to confirm that these findings were not cell type-dependent, we compared PLGA scaffolds containing live and dead MC3T3 pre-osteoblasts. Cell-seeded scaffolds were scanned on day 14 both before (Figure 2c, g, k) and after (Figure 2d, h, l) fixation. Light intensity scans of scaffold morphology showed little distinction between live (Figure 2c) and fixed (Figure 2d) cells. Phase fluctuation images, however, highlighted significant differences, with live cells (Figure 2g) displaying strong fluctuation signals, while fixed cells (Figure 2h) showed only residual noise. Overlaying the images (Figure 2k, l), it is apparent that cellular motility itself serves as an endogenous source of contrast that enables label-free monitoring of live cells within 3D scaffolds.

To further demonstrate the flexibility of motility imaging, we imaged ADSCs seeded on our PLGA scaffolds (Figure 2b, f, j) as well as on architecturally and mechanically different Algimatrix matrices (Figure 2a, e, i). The ADSCs produced a thicker tissue within the PLGA scaffolds than the MC3T3 cells had, as was apparent in both the light intensity (Figure 2f) and phase fluctuation (Figure 2j) scans. As observed via the light intensity image (Figure 2a), the morphology of the AlgiMatrix scaffold was significantly different from the PLGA scaffolds, appearing sponge-like, with thin interconnected walls. Similar to the other system, the light intensity contrast between the cells and matrix material was low, with the cells mainly distinguishable as brighter clusters within the pores. Again, it is the phase fluctuation image that emphasizes the location of the live cells (Figure 2e), with the alginate material of the scaffold itself providing little to no signal. Combining phase fluctuation and light

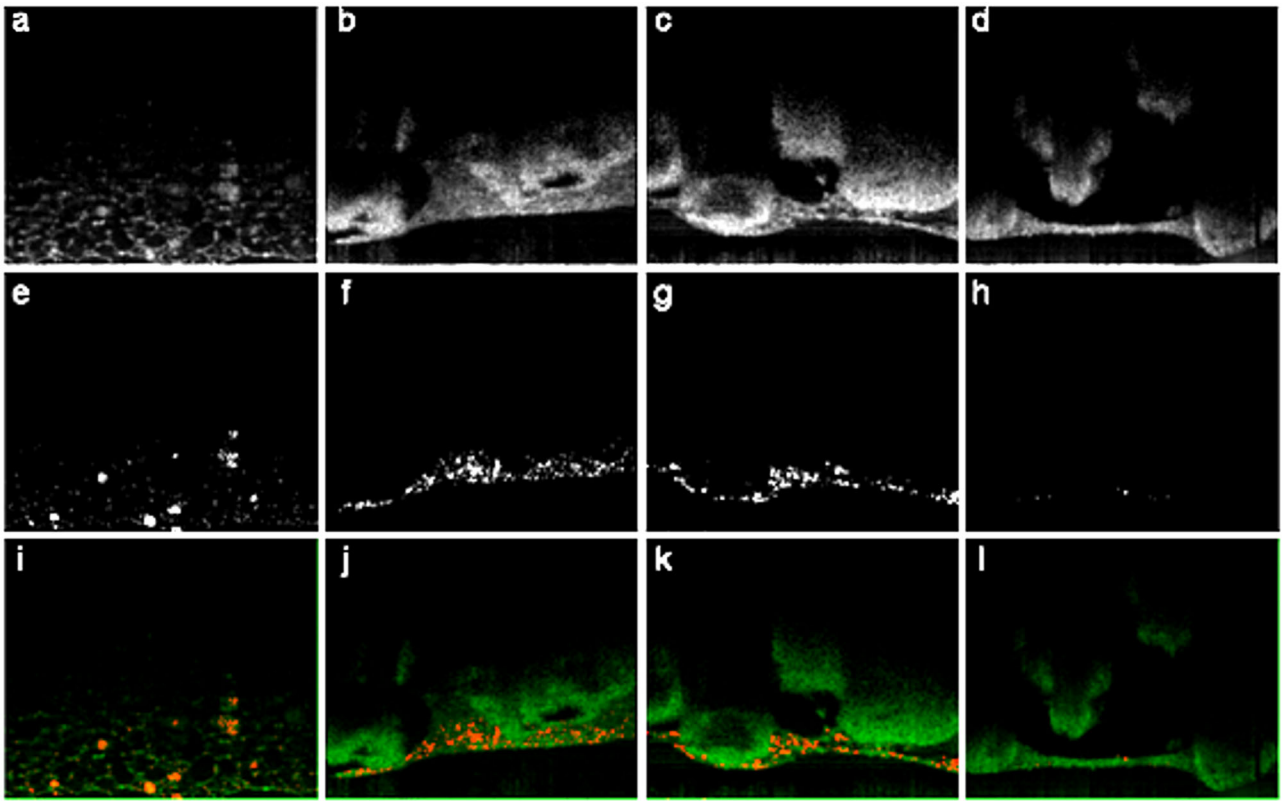

Figure 2. OCPM intensity cross-sectional images (a–d) of live adipose-derived stem cells cultured in Algimatrix (a), a commercial alginate porous scaffold, and in microplotted PLGA scaffolds (b), and compared to live (c) and fixed (d) MC3T3 cells in PLGA scaffolds, which clearly displayed the in-depth microstructure of the cell–scaffold constructs. *A priori* knowledge of the blank scaffold structure enables an estimation of the cell distribution. The corresponding phase fluctuation imaging (e–h) highlighted specific areas of the culture that were found to correspond to live cell distribution, distinguishing it from the fixed scaffold (h), where only residual noise was observed, as cells were dead and non-motile. This was clearly confirmed by cell fluctuation mapping (i–l), demonstrating the potential of OCPM for label-free and live imaging of tissue-engineering structures. All images are 1 × 1 mm

DOI: 10.1002/term

intensity scans in either engineered tissue (Figure 2i, j) once more illustrates the promise of motility imaging to provide non-invasive, real-time, label-free mapping of cell viability to overall 3D tissue morphology.

As indicated by Figure 1b, c, 3D OCPM scans offer the capability of quantifying changes in tissue volume and cell–scaffold volume ratio over time provided initial scans of unseeded scaffolds are performed. However, the estimated changes in total cell volume will also include any non-viable cells within the tissue. By contrast, motility imaging allows for the quantification of viable cell volume over time without the need for prior blank scaffold scanning, as the scaffolding material itself yields only a residual noise signal that can be corrected.

Overall, we have demonstrated that motility imaging, as achieved by our optical coherence phase microscopy (OCPM) system, creates an endogenous cell-to-scaffold contrast that enables real-time, non-invasive, label-free mapping of cellular viability to 3D tissue morphology. We have further demonstrated that this system can be used in a variety of engineered tissue systems by monitoring pre-osteoblasts and adipose-derived stem cells in two distinct scaffold systems composed of different polymers and possessing dissimilar architectures. These results, alongside the capability for quantification of viable cellular volume, highlight the great potential of motility imaging as a tool for monitoring 3D tissue growth and health within complex tissue-engineered constructs.

Acknowledgements

P.O.B. gratefully acknowledges support from the Research Councils UK for his fellowship and funding from EPSRC (Grant No. EP/G030871/1). This research was also supported by a Le Fonds Québécois de la Recherche sur la Nature et les Technologies travel grant, a National Science and Engineering Research Council of Canada Discovery Grant, and a Canadian Institutes of Health Research Regenerative Medicine Grant.

Conflict of interest

The authors have declared that there is no conflict of interest.

References

Ahearne M, Bagnaninchi PO, Yang Y, *et al*. 2008; Online monitoring of collagen fibre alignment in tissue-engineered tendon by PSOCT. *J Tissue Eng Regen Med* **2**: 521–524.

Bagnaninchi PO, Yang Y, Zghoul N, *et al*. 2007; Chitosan microchannel scaffolds for tendon tissue engineering characterized using optical coherence tomography. *Tissue Eng* **13**: 323–331.

Bagnaninchi PO, Holmes C, Drummond N, *et al*. 2011; Two-dimensional and three-dimensional viability measurements of adult stem cells with optical coherence phase microscopy. *J Biomed Opt* **16**: 086003.

Boppart SA, Bouma BE, Pitris C, *et al*. 1998; *In vivo* cellular optical coherence tomography imaging. *Nat Med* **4**: 861–865.

Choma MA, Ellerbee AK, Yang C, *et al*. 2005; Spectral-domain phase microscopy. *Opt Lett* **30**: 1162–1164.

Daoud JT, Petropavlovskaia MS, Patapas JM, *et al*. 2011; Long-term *in vitro* human pancreatic islet culture using three-dimensional microfabricated scaffolds. *Biomaterials* **32**:1536–1542.

Drexler W, Morgner U, Ghanta RK, *et al*. 2001; Ultrahigh-resolution ophthalmic optical coherence tomography. *Nat Med* **7**: 502–507.

Dunkers JP, Lee YJ, Chatterjee K. 2012; Single cell viability measurements in 3D scaffolds using *in situ* label-free imaging by optical coherence microscopy. *Biomaterials* **33**: 2119–2126.

Fujimoto JG, Brezinski ME, Tearney GJ, *et al*. 1995; Optical biopsy and imaging using optical coherence tomography. *Nat Med* **1**: 970–972.

Fujimoto JG. 2003; Optical coherence tomography for ultra-high resolution *in vivo* imaging. *Nat Biotechnol* **21**: 1361–1367.

Huang D, Swanson EA, Lin CP, *et al*. 1991; Optical coherence tomography. *Science* **254**: 1178–1181.

Jeong K, Turek JJ, Nolte DD. 2007; Volumetric motility-contrast imaging of tissue response to cytoskeletal anti-cancer drugs. *Opt Express* **15**: 14057–14064.

Liang X, Graf BW, Boppart SA. 2009; Imaging engineered tissues using structural and functional optical coherence tomography. *J Biophotonics* **2**: 643–655.

Nolte DD, An R, Turek J, *et al*. 2011; Holographic tissue dynamics spectroscopy. *J Biomed Opt* **16**: 087004.

Smith LE, Smallwood R, MacNeil S. 2010a; A comparison of optical imaging methodologies for 3D tissue engineering. *Microsc Res Tech* **73**: 1123–1133.

Smith LE, Bonesi M, Smallwood R, *et al*. 2010b; Using swept-source optical coherence tomography to monitor the formation of neo-epidermis in tissue-engineered skin. *J Tissue Eng Regen Med* **4**: 652–658.

Tan W, Oldenburg A, Norman J, *et al*. 2006; Optical coherence tomography of cell dynamics in three-dimensional tissue models. *Opt Express* **14**: 7159–7171.

Yang Y, Dubois A, Qin X, *et al*. 2006; Investigation of optical coherence tomography as an imaging modality in tissue engineering. *Phys Med Biol* **51**: 1649–1659.